

EMITTANCE EXCHANGE AT THE FERMILAB A0 PHOTOINJECTOR*

Timothy W. Koeth[#], Rutgers University, Piscataway, New Jersey, USA

Helen Edwards, Raymond P. Fliller III[†], Leo Bellantoni, Jinhao Ruan, Alex H. Lumpkin, Randy Thurman-Keup, Amber S. Johnson, Fermilab, Batavia, Illinois, USA

Abstract

An experiment to exchange the longitudinal emittance with the horizontal emittance has been installed at the Fermilab A0 Photoinjector. The exchange apparatus consists of a TM₁₁₀ deflecting mode cavity positioned between two magnetic doglegs as proposed by Kim & Sessler [1]. We report on the measurement of the emittance exchange beamline matrix elements and a direct measurement of emittance exchange.

INTRODUCTION

A transverse to longitudinal emittance exchange (EEX) has been installed at the Fermilab A0 Photoinjector for a proof-of-principle demonstration through the exchange of a larger normalized longitudinal emittance, 30 mm.mrad, with that of a smaller normalized horizontal emittance, 10 mm.mrad, of a 14.3 MeV electron beam. In this paper we report on measurements of the emittance exchange beamline matrix elements as well as a preliminary measurement of an emittance exchange.

EEX BEAMLINE & OPTICS

It is the goal of our emittance exchange experiment to exchange horizontal and longitudinal emittances of an electron beam. The apparatus that we have developed, which is a variant of Kim and Sessler's proposal, can be easily described through a linear optics treatment of the exchange beamline [1]. We describe the entire exchange apparatus by a typical 4x4 matrix relating the horizontal and longitudinal parameters, Δx , $\Delta x'$, Δz , $\Delta \delta$ ($\delta = \Delta p/p$):

$$M_{EEX} = \begin{pmatrix} A_{11} & A_{12} & B_{11} & B_{12} \\ A_{21} & A_{22} & B_{21} & B_{22} \\ C_{11} & C_{12} & D_{11} & D_{12} \\ C_{21} & C_{22} & D_{21} & D_{22} \end{pmatrix}$$

A complete exchange matrix would be one in which the elements of the A and D sub-blocks become zero and the B and C sub-blocks become populated.

The A0 Photoinjector EEX apparatus, outlined in Fig. 1, consists of a 3.9 GHz TM₁₁₀ deflecting mode cavity located between two 'dogleg' magnetic channels. The TM₁₁₀ deflecting mode cavity is a LN₂ cooled, normal conducting, variant of a superconducting version

previously developed at Fermilab [2]. The longitudinal electric field of the TM₁₁₀ mode is zero on axis and grows linearly off axis, the vertical magnetic field produces a time dependent transverse kick with respect to the synchronous particle. The TM₁₁₀ deflecting mode cavity's strength, k , is given by:

$$k = \frac{eV_{\perp}\omega}{Ec},$$

where V_{\perp} is the peak deflecting field normalized to the beam energy, E , and ω is the resonant frequency.

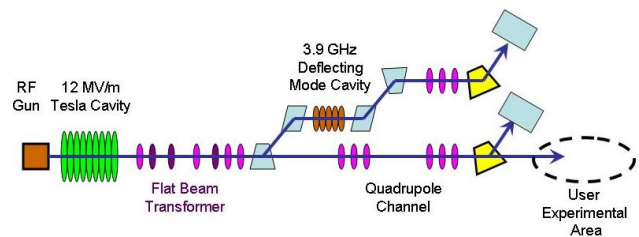


Figure 1: Layout of the A0 Photoinjector with straight ahead and EEX beamline sections.

Using a thin lens approximation of a cavity immediately between two magnetic doglegs, we can analytically express our EEX beamline matrix as:

$$\begin{pmatrix} 1+Dk & L+Dk+(1+Dk)L & kL & D+D(1+Dk)+\alpha DkL \\ 0 & 1+Dk & k & \alpha Dk \\ \alpha Dk & D+D(1+Dk)+\alpha DkL & 1+Dk & \alpha D+\alpha D^2k+\alpha D(1+Dk) \\ k & kL & 0 & 1+Dk \end{pmatrix}$$

where L is the drift between two magnetic dipoles that form a magnetic dogleg and D is the dispersion generated by one dogleg, and α is the magnitude of the bend angle.

It can easily be seen that in the special case where the TM₁₁₀ cavity strength, k , (defined 100% at 3.03 m⁻¹ in our case) equals the negative reciprocal of the dispersion, D , (0.33 m in our case) the diagonal sub-blocks of the matrix become zero while the off-diagonal sub-blocks become populated. Our bending angle is 22.5°.

$$M_{EEX} = \begin{pmatrix} 0 & 0 & -\frac{1}{D} & 0 \\ 0 & 0 & -\frac{1}{D} & -\alpha \\ -\alpha & 0 & 0 & 0 \\ -\frac{1}{D} & -\frac{1}{\alpha} & 0 & 0 \end{pmatrix}$$

In practice, due to the finite length of our TM₁₁₀ deflecting mode cavity, several of the on-diagonal block elements are left non zero [3]. This, in addition to other higher order effects, such as space charge and CSR, will lead to an imperfect exchange and a coupling of the final emittances [4].

* This manuscript has been authored by Fermi Research Alliance, LLC under Contract No. DE-AC02-07CH11359 with the U.S. Department of Energy.

[#]koeth@physics.rutgers.edu

[†]Present address: NSLS II Project, Brookhaven National Laboratory, Upton, NY, 11973-5000NY

EEX BEAMLINE DIAGNOSTICS

The EEX beam line is outfitted with ten Beam Position Monitors (BPM); the transverse beam profiles are measured by eight Optical Transition Radiation (OTR) viewing screens along the beamline. Two sets of tungsten slits and YAG viewing screen pairs measure the transverse beam divergence before and after the exchange beamline. EEX input and output central momenta and momentum spreads are measured by two spectrometer magnets and viewing screens. A single Hamamatsu C5680 streak camera outfitted with a synchroscan unit provides a measurement of the laser pulse length, electron bunch lengths at the input and output of the exchanger, and changes in bunch time-of-arrival at the picosecond level [5]. Finally, a Martin-Puplett interferometer is installed at the end of the EEX beamline to perform sub-picosecond bunch length measurements [6].

EEX MATRIX MEASUREMENT

To verify the expected transport matrix, difference orbits have been used to measure the EEX beamline matrix. Diagnostic limitations required the measured matrix elements include the 2.1 m drift prior to the first EEX dipole magnet and the 0.2 m drift after the fourth EEX dipole. The procedure was to establish a nominal 14.3 MeV beam orbit through the EEX beamline and measure both the 6-D input and output vectors. Then one of the 6-D input vector's elements was varied; the change in the 6-D output vector was measured. To demonstrate the "turn-on" evolution of the EEX matrix, this procedure was repeated with the TM_{110} deflecting mode cavity off, at the full strength for the complete EEX condition, and at three intermediate strengths. The BPM readings gave Δx , $\Delta x'$, Δy , and $\Delta y'$ data, while the streak camera provided the Δz information, and finally the vertical bending spectrometer

in conjunction with the subsequent vertical BPM position reading provided the output $\Delta\delta$ data.

Figure 2 graphically displays the 4x4 transport matrix as a function of the TM_{110} deflecting mode cavity strength. The TM_{110} cavity is completely off at 0% and is energized to the optimal level for EEX in our beamline at 100%. The measurements (circles) are compared to a simple linear optics model displayed by the red line. For the most part, we see close agreement. Although not shown, the full 6x6 transport matrix was measured. The corresponding vertical plane elements, as expected, displayed no dependence on the TM_{110} cavity's state.

We consider the measurements of the second column "pure" in the sense that by use of a single correction dipole we can obtain an input angle without a transverse offset at a prescribed longitudinal location. However, due to the manual nature of setting two longitudinally spaced correctors to generate a horizontal input offset, Δx , it is impossible to avoid an input angle as well. By first measuring the respective input $\Delta x'$ dependencies and having the ability to measure the input angle, we subtract off the angular component from the input Δx measurements. A similar circumstance occurs in the measurement of the third and fourth columns. The input $\Delta\delta$ is simply controlled by adjusting the Photoinjector's capture cavity gradient, and thus is also considered a "pure" measurement. The third column is a measure of the output vector's dependence on the input beams Δz w.r.t. the synchronous bunch, i.e. time of arrival differences. To avoid the complexities of adjusting the Photoinjector's timed supply of electron bunches the phase of the TM_{110} cavity was simply adjusted to affect differing bunch time-of-arrival. Except for the TM_{110} cavity, all of the EEX components are static, thus a phase advance of 1° of the TM_{110} cavity is equivalent to 0.7 ps earlier arrival time, or a 0.2 mm longitudinal offset.

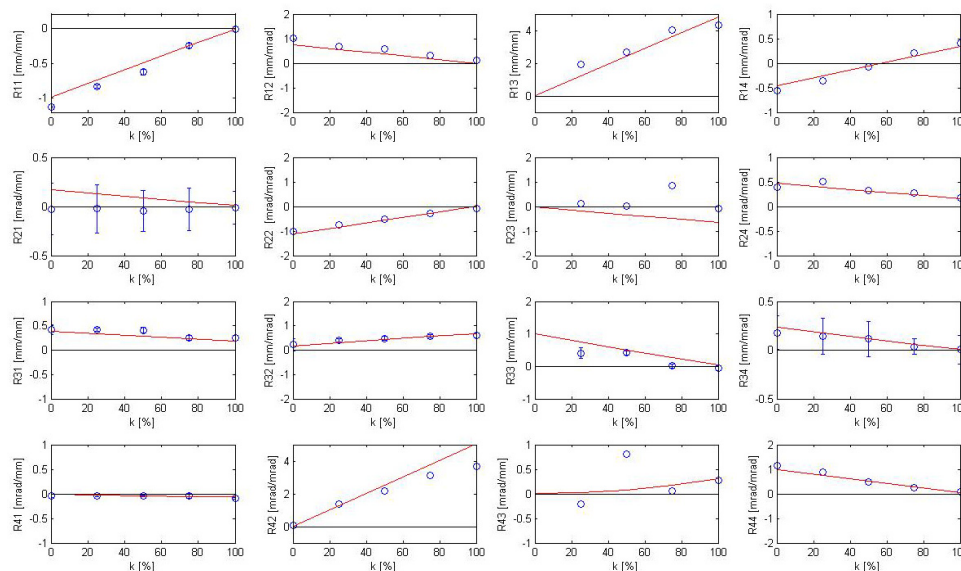


Figure 2: Measurement of 4x4 (horizontal and longitudinal) EEX matrix evolution as the TM_{110} cavity strength is ramped from 0%, off, to 100%, full EEX strength. The red traces are expected values from a linear optics model. The analysis is presently still in progress thus not all measurements display error bars.

Simply adjusting the TM_{110} deflecting mode cavity phase comes at the cost of losing the 0%, cavity off, data points. Several of the third column data points have large error bars as a result of the measurements relatively strong sensitivities to slight fluctuations of input parameters other than the one intentionally being adjusted. For instance the R43 element has a large uncertainty at the 50% data point. At the TM_{110} cavity 50% level, any input momentum jitter is propagated through to the measurement point at half amplitude, and can swamp the signal sought. A future analysis will account for this energy jitter by using the horizontal BPM reading directly before the TM_{110} deflecting cavity as a spectrometer, thus enabling us to remove the effect of the energy offset on a shot-to-shot basis.

DIRECT EEX MEASUREMENT

A direct measurement of emittance exchange with a low charge 14.3 MeV beam consisting of 80 bunches per RF pulse was performed. The bunch charge of 250 pC was chosen as compromise between diagnostic requirements and space charge effects. Simulations provided an initial starting point for input beam conditions, including quadrupole settings and beam chirp [5]. The input horizontal parameter space was varied by adjusting two input quads while the output energy spread and bunch lengths were measured. Sub-picosecond bunch lengths, as well as very small energy spreads, ~ 10 keV, could be obtained; however, not simultaneously. Several output parameters have been mapped against the input quads strengths. The first is a map of the interferometer’s pyroelectric detectors sum signal, thus, an un-calibrated reference signal that is inversely proportional to bunch length, shown in Fig. 3.

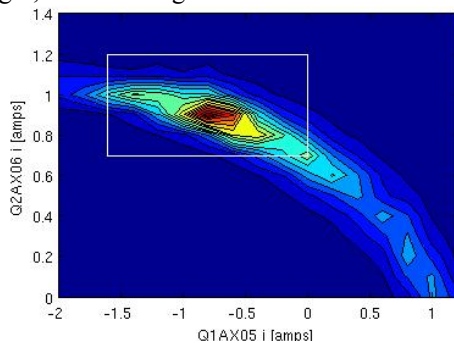


Figure 3: A relative output bunch length mapped against two input quad settings. (dark red is the minimum bunch length). The white box outlines Fig. 4 boundary.

Subsequent measurements at the location of the peak pyroelectric signal yielded a bunch length that was below the resolution limit of the streak camera and at which the interferometer revealed a bunch length of 0.40 ± 0.04 ps rms. Output energy spread measurements at the same location yielded approximately 110keV.

An energy spread map near the peak pyroelectric signal was generated and is shown in Fig. 4.

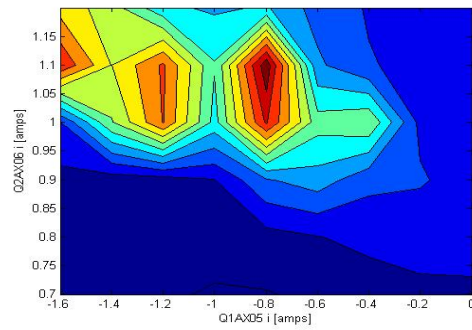


Figure 4: Output energy spread mapped against input quads. (dark blue are lowest energy spreads).

Guided by these maps, the input quads were empirically adjusted to find a location where the energy spread and bunch length product yielded a minimum output ϵ_z , at which an entire input and output emittance data set was taken; the normalized preliminary emittance exchange results are summarized in Table 1. We were unable to measure TM_{110} cavity off ϵ_x point as the output horizontal beam spot size is larger than the viewing screen. We are investigating the large increase in ϵ_y in the TM_{110} cavity on case.

Table 1: Preliminary EEX Data Set

	ϵ_x mm.mrad	ϵ_y mm.mrad	ϵ_z mm.mrad
INPUT	9.2	7.2	32.5
out TM_{110} off	N/A	11.4	N/A
out TM_{110} on	38.4	18.2	13.3

CONCLUSIONS

A measurement of our EEX transport matrix has been completed and demonstrates the desired properties of an EEX beamline. Additionally, an initial direct emittance exchange has been performed, but due to the large parameter space, will require further investigation.

REFERENCES

- [1] K.-J. Kim and A. Sessler, AIP Conf. Proc. **821**, 115(2006).
- [2] T.W. Koeth, et. Al, “A Copper 3.9 GHz TM_{110} Cavity for Emittance Exchange” Proceedings of PAC 2007, Albuquerque, New Mexico, THPAS079.
- [3] D. A. Edwards. Unpublished.
- [4] R. P. Fliller III “Start to End Simulations of Transverse to Longitudinal Emittance Exchange at the A0 Photoinjector”, EPAC08, Paper THPC014.
- [5] A. H. Lumpkin, et al., “Initial Synchroscan Streak Camera Imaging at the A0 Photoinjector,” Proceedings of 2008 Beam Instrumentation Workshop, Lake Tahoe, CA, USA.
- [6] R. Thurman-Keup, et al., "Bunch Length Measurement at the Fermilab A0 Photoinjector using a Martin Puplett Interferometer", Proceedings of 2008 Beam Instrumentation Workshop, Lake Tahoe, CA, USA.